

zPROBE: Zero Peek Robustness Checks for Federated Learning

Zahra Ghodsi^{1*}, Mojan Javaheripi^{1*}, Nojan Sheybani^{1*}, Xinqiao Zhang^{1*},
Ke Huang², Farinaz Koushanfar¹

¹University of California San Diego, ²San Diego State University

¹{zghodsi, mojan, nsheyban, x5zhang, farinaz}@ucsd.edu

²khuang@sdsu.edu

Abstract

Privacy-preserving federated learning allows multiple users to jointly train a model with coordination of a central server. The server only learns the final aggregation result, thus the users' (private) training data is not leaked from the individual model updates. However, keeping the individual updates private allows malicious users to perform *Byzantine attacks* and degrade the accuracy without being detected. Best existing defenses against Byzantine workers rely on robust rank-based statistics, e.g., median, to find malicious updates. However, implementing privacy-preserving rank-based statistics is nontrivial and not scalable in the secure domain, as it requires sorting all individual updates. We establish the first private robustness check that uses high break point rank-based statistics on aggregated model updates. By exploiting randomized clustering, we significantly improve the scalability of our defense without compromising privacy. We leverage our statistical bounds in zero-knowledge proofs to detect and remove malicious updates without revealing the private user updates. Our novel framework, zPROBE, enables Byzantine resilient and secure federated learning. Empirical evaluations demonstrate that zPROBE provides a low overhead solution to defend against state-of-the-art Byzantine attacks while preserving privacy.

1 Introduction

Federated learning (FL) has emerged as a popular paradigm for training a central model on a dataset distributed amongst many parties, by sending model updates and without requiring the parties to share their data. However, model updates in FL can be exploited by adversaries to infer properties of the users' private training data (Melis et al. 2019). This lack of privacy prohibits the use of FL in many machine learning applications that involve sensitive data such as healthcare information (Rieke et al. 2020; Xu et al. 2021) or financial transactions (Yang et al. 2019). As such, existing FL schemes are augmented with privacy-preserving guarantees. Recent work propose secure aggregation protocols using cryptography (Bonawitz et al. 2017; Bell et al. 2020; Truex et al. 2019). In these protocols, the server does not learn individual user updates, but only a final aggregate with contribution from several users. Hiding individual updates from the server opens a large attack surface for malicious clients to send invalid updates that compromise the integrity of distributed training.

Byzantine attacks on FL are carried out by malicious clients who manipulate their local updates to degrade the model performance (Damaskinos et al. 2018; Bhagoji et al. 2019; Baruch et al. 2019). Popular high-fidelity Byzantine-robust aggregation rules rely on rank-based statistics, e.g., trimmed mean (Yin et al. 2018; Xie et al. 2018b), median (Yin et al. 2018), mean around median (Xie et al. 2018a; Boussetta et al. 2021), and geometric median (Chen et al. 2017; Guerroui et al. 2018; Xie et al. 2018a). These schemes require sorting of the individual model updates across users. As such, using them in secure FL is nontrivial and unscalable to large number of users since the central server cannot access the (plaintext) value of user updates.

In this work we address aforementioned challenges and provide high break point Byzantine tolerance using rank-based statistics while preserving privacy. We propose a median-based robustness check that derives a threshold for acceptable model updates using securely computed mean over random user clusters. Our thresholds are dynamic and automatically change based on the distribution of the gradients. Notably, we do not need access to individual user updates or public datasets to establish our defense. We leverage the computed thresholds to identify and filter malicious users in a privacy-preserving manner. Our Byzantine-robust framework, zPROBE, incorporates carefully crafted zero-knowledge proofs (Weng et al. 2021a,b) to check user behavior and identify possible malicious actions, including sending Byzantine updates or deviating from the secure aggregation protocol. As such, zPROBE guarantees correct and consistent behavior in the challenging malicious threat model.

We incorporate probabilistic optimizations in the design of zPROBE to minimize the overhead of our zero-knowledge checks, without compromising security. By co-designing the robustness defense and cryptographic components of zPROBE, we are able to provide a scalable and low overhead solution for private and robust FL. Our construction is the first of its kind with cost that grows sub-linearly with respect to the number of clients. zPROBE performs an aggregation round on ResNet20 over CIFAR-10 with only sub-second client compute time. In summary, our contributions are:

- Developing a novel privacy-preserving robustness check based on rank-based statistics. zPROBE is robust against various Byzantine attacks with 0.5–2.8% higher accuracy compared to prior work on private and robust FL.

*These authors contributed equally.

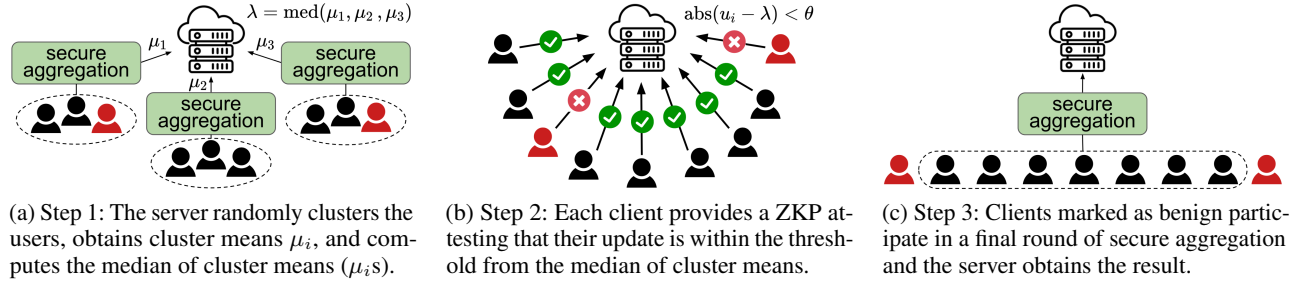


Figure 1: High level description of zPROBE robust and private aggregation.

- Enabling private and robust aggregation in the malicious threat model by incorporating zero-knowledge proofs. Our Byzantine-robust secure aggregation, for the first time, scales sub-linearly with respect to number of clients.
- Leveraging probabilistic optimizations to reduce zPROBE overhead without compromising security, resulting in orders of magnitude client runtime reduction.

2 Cryptographic Primitives

Shamir Secret Sharing (Shamir 1979) is a method to distribute a secret s between n parties such that any t shares can be used to reconstruct s , but any set of $t - 1$ or fewer shares reveal no information about the secret. Shamir’s scheme picks a random $(t - 1)$ -degree polynomial P such that $P(0) = s$. The shares are then created as $(i, P(i)), i \in \{1, \dots, n\}$. With t shares, Lagrange Interpolation can be used to reconstruct the polynomial and obtain the secret.

Zero-Knowledge Proof (ZKP) is a cryptographic primitive between two parties, a prover \mathcal{P} and a verifier \mathcal{V} , which allows \mathcal{P} to convince \mathcal{V} that a computation on \mathcal{P} ’s private inputs is correct without revealing the inputs. We use the Wolverine protocol (Weng et al. 2021a) with highly efficient \mathcal{P} in terms of runtime, memory usage, and communication. In Wolverine, value x known by \mathcal{P} can be authenticated using information-theoretic message authentication codes (IT-MACs) (Damgård et al. 2012) as follows: assume Δ is a global key sampled uniformly and is known only to \mathcal{V} . \mathcal{V} is given a uniform key $K[x]$ and \mathcal{P} is given the corresponding MAC tag $M[x] = K[x] + \Delta \cdot x$. An authenticated value can be *opened* (verified) by \mathcal{P} sending x and $M[x]$ to \mathcal{V} to check whether $M[x] \stackrel{?}{=} K[x] + \Delta \cdot x$. Wolverine represents the computation as an arithmetic or Boolean circuit, for which the secret wire values are authenticated as described. The circuit is evaluated jointly by \mathcal{P} and \mathcal{V} , at the end of which \mathcal{P} opens the output indicating the proof correctness.

Secure FL Aggregation includes a server and n clients each holding a private vector of model updates with l parameters $\mathbf{u} \in \mathbb{R}^l$. The server wishes to obtain the aggregate $\sum_{i=1}^n \mathbf{u}_i$ without learning any of the individual client updates. (Bonawitz et al. 2017) and follow up (Bell et al. 2020) propose a secure aggregation protocol using low-overhead cryptographic primitives such as one-time pads. Each pair of clients (i, j) agree on a random vector $\mathbf{m}_{i,j}$. User i adds $\mathbf{m}_{i,j}$ to their input, and user j subtracts it from their input so

the masks cancel out when aggregated. To ensure privacy in case of dropout or network delays, each user adds an additional random mask \mathbf{r}_i . Users then create t -out-of- n Shamir shares of their masks and share them with other clients. User i computes their masked input as follows:

$$\mathbf{v}_i = \mathbf{u}_i + \mathbf{r}_i - \sum_{0 < j < i} \mathbf{m}_{i,j} + \sum_{i < j \leq n} \mathbf{m}_{i,j} \quad (1)$$

Once the server receives all masked inputs, it asks for shares of pairwise masks for dropped users and shares of individual masks for surviving users (but never both) to reconstruct the aggregate value. The construction in (Bell et al. 2020) builds over (Bonawitz et al. 2017) and improves the client runtime complexity to logarithmic scale rather than linear with respect to the number of clients. Note that the secure aggregation of (Bell et al. 2020; Bonawitz et al. 2017) assumes the clients are semi-honest and do not deviate from the protocol. However, these assumptions are not suitable for our threat model which involves malicious clients. We propose an aggregation protocol that benefits from speedups in (Bell et al. 2020) and is augmented with zero-knowledge proofs for the challenging malicious setting as described below.

3 Methodology

Threat Model. We aim to protect the privacy of individual client updates as they leak information about clients’ private training data. No party should learn any information about a client’s update other than the contribution to an aggregate value with inputs from a large number of other clients. We also aim to protect the central model against Byzantine attacks, i.e., when a malicious client sends invalid updates to degrade the model performance. We consider a semi-honest server that follows the protocol but may try to learn more information from the received data. We assume a portion of clients are malicious, i.e., arbitrarily deviating from the protocol, or sending erroneous updates to cause divergence in the central model. Notably, we assume the clients may:

- ① perform Byzantine attacks by changing the value of their model update to degrade central model performance,
- ② use inconsistent update values in different steps of the secure aggregation protocol,
- ③ perform the masked update computation in Eq. 1 incorrectly or with wrong values, and
- ④ use incorrect seed values in generating masks and shares.

To the best of our knowledge, zPROBE is the first single-server

Algorithm 1: zPROBE secure aggregation

Input: Shamir threshold value t , clients set U
Round 1: Mask Generation
client i : Generate key pair (sk_i, pk_i) , sample b_i
 $a_{i,j} \leftarrow \text{KeyAgreement}(sk_i, pk_j)$
 $m_{i,j} \leftarrow \text{PRG}(a_{i,j})$, $r_i \leftarrow \text{PRG}(b_i)$
 $\{s_j^{sk}\}_{j \in U} \leftarrow \text{SS}(sk_i, t)$, $\{s_j^b\}_{j \in U} \leftarrow \text{SS}(b_i, t)$
Send s_j^{sk} , s_j^b to client j
Round 2: Update Masking
client i : $v_i \leftarrow u_i + r_i - \sum_{0 < j < i} m_{i,j} + \sum_{i < j \leq U} m_{i,j}$
Authenticate u_i and send v_i to server
Perform correctness check in Alg 2
server: Sample q indices S_i (Sec. 3.4) for client i
Perform correctness check in Alg 2
Round 3: Aggregate Unmasking
server: $U_d \leftarrow$ dropped clients, $U_s \leftarrow$ surviving clients
Collect t shares of $\{s_i^{sk}\}_{i \in U_d}$ and $\{s_i^b\}_{i \in U_s}$
 $\text{Agg} \leftarrow \sum_{i \in U_s} v_i - \sum_{i \in U_s} r_i + \sum_{i \in U_s, j \in U_d} m_{i,j}$

framework with malicious clients that is resilient against such an extensive attack surface, supports client dropouts, and does not require a public clean dataset.

3.1 zPROBE Overview

zPROBE comprises two main components, namely, secure aggregation, and robustness establishment. We propose a new secure aggregation protocol for malicious clients in Sec. 3.2. Our proposed method to establish robustness is detailed in Sec. 3.3. We design an adaptive Byzantine defense that finds the dynamic range of acceptable model updates per iteration. Using the derived bounds, we perform a secure range check on client updates to filter Byzantine attackers. Our robustness check is privacy-preserving and highly scalable.

The proposed robust and private aggregation is performed in three steps as illustrated in Fig. 1. First the server clusters the clients randomly into c clusters. Each cluster c_j then performs zPROBE’s secure aggregation protocol. The server obtains the aggregate value α_j and the mean $\mu_j = \alpha_j/|c_j|$ for each cluster in plaintext. In the second step, the server uses the median λ of all cluster means to compute a threshold θ for model updates. The values of median λ and threshold θ are public, and broadcasted by the server to all clients. Each client i then provides a zero-knowledge proof attesting that their update is within the threshold from the median, i.e., $\text{abs}(u_i - \lambda) < \theta$. This ensures that clients are not performing Byzantine attacks on the central model (item ① in threat model). Users that fail to provide the proof are considered malicious and treated as dropped. The remaining users participate in a round of zPROBE secure aggregation and the server obtains the final aggregate result.

3.2 zPROBE Secure Aggregation

Alg. 1 shows the detailed steps for zPROBE’s secure aggregation for n clients consisting of three rounds. In round 1, each client i generates a key pair (sk_i, pk_i) , samples a random

Algorithm 2: Circuit for zPROBE correctness check

Client input: $b_i, a_{i,j}$, authenticated u_i
Public input: v_i , indices set S_i , clients set U
 $check = 1$
for k in S_i
 $\hat{r}_i^k \leftarrow \text{PRG}^k(b_i)$
for j in U
 $\hat{m}_{i,j}^k \leftarrow \text{PRG}^k(a_{i,j})$
 $\hat{v}_i^k \leftarrow u_i^k + \hat{r}_i^k - \sum_{0 < j < i} \hat{m}_{i,j}^k + \sum_{i < j \leq n} \hat{m}_{i,j}^k$
 $check = check \wedge (\hat{v}_i^k = v_i^k)$
return $check$

Algorithm 3: Circuit for zPROBE robustness check

Client input: Authenticated u_i
Public input: λ, θ , indices set S_i
 $check = 1$
for k in S_i
 $check = check \wedge (|u_i^k - \lambda^k| < \theta^k)$
return $check$

seed b_i , and performs a key agreement protocol (Diffie and Hellman 1976) with client j to obtain a shared seed $a_{i,j}$. The seeds are used to generate individual and pairwise masks using a pseudorandom generator (PRG). Each client then creates t -out-of- n Shamir shares (SS) of sk_i and b_i , and sends one share of each to every other client.

In the second round, each client uses the masks generated in round one to compute masked updates according to Eq. 1, which are then sent to the server. All clients perform the ZKP authentication protocol described in Sec. 2 on their update. This ensures that clients use consistent update values across different steps (item ② in threat model). In addition, each client proves, in zero-knowledge, that their sent value v_i is correctly computed as shown in Alg. 2. Specifically, the circuit that is evaluated in zero-knowledge expands the generated seeds to masks, and computes the masked update using Eq. 1. The value of $check$ is then opened by the client, and the server verifies that $check = 1$. This ensures that the masks are correctly generated from seeds, and the masked update is correctly computed (item ③ in the threat model). Users that fail to provide the proof are dropped in the next round and their update is not incorporated in aggregation.

We introduce optimizations in Sec 3.4 that allow the server to derive a bound q , for the number of model updates to be checked, such that the probability of detecting Byzantine updates is higher than a predefined rate. The server samples q random parameters from client i , and performs the update correctness check (Alg. 2). We note that clients are not motivated to modify the seeds for creating masks, since this results in uncontrollable, out-of-bound errors that can be easily detected by the server (item ④ in threat model). We discuss the effect of using wrong seeds in Appendix A.

In round 3, the server performs unmasking by asking for shares of sk_i for dropped users and shares of b_i for surviving users, which are then used to reconstruct the pairwise and individual masks for dropped and surviving users respectively. The server is then able to obtain the aggregate result.

3.3 Establishing Robustness

Deriving Dynamic Bounds. To identify the malicious gradient updates, we adaptively find the valid range for *acceptable* gradients per iteration. In this context, acceptable gradients are those that do not harm the central model’s convergence when included in the gradient aggregation. To successfully identify such gradients, we rely on the underlying assumption that benign model updates are in the majority while harmful Byzantine updates form a minority of outlier values. In the presence of outliers, the median can serve as a reliable baseline for in-distribution values (Boussetta et al. 2021).

In the secure FL setup, the true value of the individual user updates is not revealed to the server. Calculating the median on the masked user updates is therefore nontrivial since it requires sorting the values which incurs extremely high overheads in secure domain. We circumvent this challenge by forming clusters of users, where our secure aggregation can be used to efficiently compute the average of their updates. The secure aggregation abstracts out the user’s individual updates, but reveals the final mean value for each cluster $\{\mu_1, \mu_2, \dots, \mu_c\}$ to the server. The server can thus easily compute the median (λ) on the mean of clusters in plaintext.

Using the Central Limit Theorem for Sums, cluster means follow a normal distribution $\mu_i \sim \mathcal{N}(\mu, \frac{1}{\sqrt{n_c}}\sigma)$ where μ and σ denote the mean and standard deviation of the original model updates and n_c is the cluster size. We can thus use the standard deviation of the cluster means (σ_μ) as a distance metric for marking outlier updates. The distance is measured from the median of means λ , which serves as an acceptable model update drawn from $\mathcal{N}(\mu, \frac{1}{\sqrt{n_c}}\sigma)$. For a given update u_i , we investigate Byzantine behavior by checking $|u_i - \lambda| < \theta$, where $\theta = \eta \cdot \sigma_\mu = \frac{\eta}{\sqrt{n_c}}\sigma$. The value of η can be tuned based on cluster size (n_c) and the desired statistical bounds on the distance in terms of the standard deviation of model updates (σ). Specifically, assuming a higher bound on the portion of malicious users ϕ_{max} , the server can automatically adjust η such that at most $(1 - \phi_{max}) \cdot n$ of the users are marked as benign where n is the total user count.

Secure Robustness Check. We use ZKPs to identify malicious clients that send invalid updates, without compromising clients’ privacy. Our ZKP relies on the robustness metrics derived in Sec. 3.3, i.e., the median of cluster means λ and the threshold θ . Clients (\mathcal{P}) prove to the server (\mathcal{V}) that their updates comply with the robustness range check.

During the aggregation round in step 1, clients authenticate their private updates, and the authenticated value is used in steps 2 and 3. This ensures that consistent values are used across steps and clients can not change their update after learning λ and θ to fit in the robustness threshold. In step 2, the server makes λ and θ public. Inside ZKP, the clients’ updates u_i are used in a Boolean circuit determining if $|u_i - \lambda| < \theta$ as outlined in Alg. 3. Invalid model updates that fail the range check are dropped from the final aggregation round.

3.4 Probabilistic Optimizations

This section provides statistical bounds on the number of required checks to accurately detect malicious clients. Using

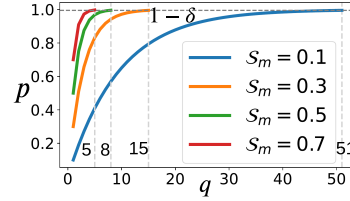


Figure 2: Detection probability vs. number of ZKP checks (q). Vertical lines mark the required q values for 99.5% detection rate.

the derived bounds, we optimize our framework for minimum overhead, thereby ensuring scalability to large models.

Malicious clients can compromise their update, by sending updates with distance margins larger than the tolerable threshold θ , or sending incorrect masked updates (Eq. 1). Assume that a portion of model updates S_m , are compromised. The probability of detecting a malicious update is equivalent to finding at least one compromised parameter gradient:

$$p = 1 - \binom{l \cdot (1 - S_m)}{q} / \binom{l}{q}, \quad (2)$$

where l is the total model parameter updates, and q denotes the number of per-user ZKP checks on model updates. The above formulation confirms that it is indeed not necessary to perform ZKP checks on all parameter updates within the model. Rather, q can be easily computed via Eq. 2, such that the probability of detecting a compromised update is higher than a predefined rate: $p > 1 - \delta$. Fig. 2 shows the probability of detecting malicious users versus number of ZKP checks for a model with $l = 60K$ parameters. As seen, zPROBE guarantees a failure rate lower than $\delta = 0.005$ with very few ZKP checks. Note that malicious users are incentivized to attack a high portion of updates to increase their effect on the aggregated model’s accuracy. We leverage Eq. 2 to derive the required number of correctness and robustness checks as described in Alg. 2 and Alg. 3. For each check, the server computes the bound q , then samples q random indices from model parameters for each client. The clients then provide ZKPs for the selected set of parameter indices.

4 Experiments

4.1 Experimental Setup

We provide details about the benchmarked models, datasets, and defense implementation in Appendix B.

Byzantine Attacks. We assume 25% of the clients are Byzantine, which is a common assumption in the literature (Baruch et al. 2019). Malicious users alter a portion S_m of benign model updates and masks according to a Byzantine attack scenario. We show the effectiveness of our robustness checks against three commonly observed Byzantine attack scenarios: *Sign Flip* (Damaskinos et al. 2018), *Scaling* (Bhagoji et al. 2019), and *Non-omniscient attack* (Baruch et al. 2019). Attack details are included in Appendix C.

Baseline Defenses. We present comparisons with prior work on robust and private FL, i.e., BREA (So et al. 2020) and EIFFeL (Chowdhury et al. 2021). While zPROBE is able to implement popular defenses based on rank-based statistics, EIFFeL is limited to static thresholds and requires access to clean public datasets. BREA implements multi-Krum (Damaskinos et al. 2019), but leaks pairwise distances

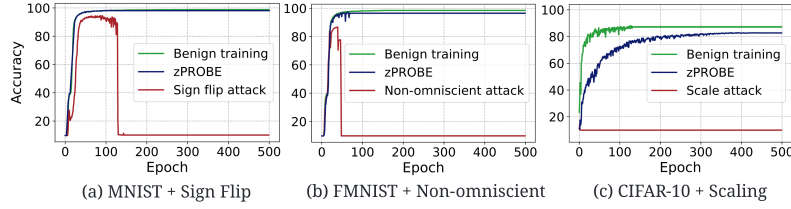


Figure 3: Test accuracy vs. FL training epochs for different attacks and benchmarks. Each plot shows the benign training (green), Byzantine training without defense (maroon), and Byzantine training with zPROBE defense.

Aggregator	IID	non-IID
AVG	93.2 \pm 0.2	92.7 \pm 0.3
KRUM	91.6 \pm 0.3	53.1 \pm 3.9
CM	91.9 \pm 0.2	78.6 \pm 3.1
CCLip	93.0 \pm 0.2	91.2 \pm 0.5
RFA	93.2 \pm 0.2	92.6 \pm 0.2
zPROBE	99.0 \pm 0.0	98.6 \pm 0.4

Table 1: zPROBE and previous robust FL aggregators for non-IID data, accuracy reported across 10 runs.

of clients to the server. zPROBE achieves lower computation complexity compared to both works and higher accuracy¹ compared to EIFFeL. We also benchmark a commonly used aggregator which uses only the median of cluster means, and show that it results in drastic loss of accuracy compared to zPROBE. Additionally, we evaluate zPROBE when the training data is non-IID and show our adaptive bounds outperform the state-of-the-art defense in (Karimireddy et al. 2022)².

4.2 Defense Performance

IID Training Data. We evaluate zPROBE on various benchmarks using $n = 50$ clients picked for a training round, randomly grouped into $c = 7$ clusters. In Section 4.4 we present evaluations with different number of clients between 30 and 200. Consistent with prior work (Baruch et al. 2019), we assume malicious users compromise all model updates to maximize the degradation of the central model’s accuracy. Fig. 3 demonstrates the convergence behavior of the FL scheme in the presence of Byzantine users with and without zPROBE defense. As seen, zPROBE successfully eliminates the effect of malicious model updates and recovers the ground-truth accuracy. We show evaluations of zPROBE accuracy on other variants of the dataset and attack in Fig. 7 in Appendix D. On the MNIST benchmark, the byzantine attacks cause the central model’s accuracy to reduce to nearly random guess (10.2%-11.2%), without any defense. zPROBE successfully thwarts the malicious updates, recovering benign accuracy within 0.0%-0.6% margin. On F-MNIST, we recover the original $\sim 88\%$ drop of accuracy caused by the attacks to 0%-2% drop. Finally, on CIFAR-10, the gap between benign training and the attacked model is reduced from 45%-90% to only 3%-7%. Compared to EIFFeL (Chowdhury et al. 2021), zPROBE achieves 1.2%, 0.5%, and 2.8% higher accuracy when evaluated on the same attack applied to MNIST, FMNIST, and CIFAR-10, respectively.

Non-IID Training Data. Most recently, Karimireddy et al. (2022) show user clustering over existing robust aggregation methods can adapt them to heterogeneous (non-IID) data. We follow their training setup and hyperparameters to distribute the MNIST dataset unevenly across 25 users. As shown in Tab. 1, zPROBE defense outperforms the accuracies

obtained by the various defenses evaluated in (Karimireddy et al. 2022). This performance boost we believe can be attributed to 1) the use of rank-based statistics to establish dynamic thresholds, and 2) the use of all benign gradients in the aggregation, rather than replacing all values with a robust aggregator, e.g., as in KRUM.

4.3 Runtime and Complexity Analysis

Tab. 2 summarizes the total runtime for clients in zPROBE for one round of federated training with $n = 50$, $c = 7$, and $\mathcal{S}_m = 0.3$ across different benchmarks. We use the secure aggregation protocol of (Bell et al. 2020) as our baseline, which does not provide security against malicious clients or robustness against Byzantine attacks. We show the effect of \mathcal{S}_m on zPROBE runtime in Tab. 5 in Appendix E. We also show the effect of increasing the number of clients n on zPROBE runtime in Tab. 6 in Appendix F.

In Tab. 2, we can see that as the underlying model gets much larger (growing $\sim 4\times$ in size from the MNIST to CIFAR-10 tasks) zPROBE overhead grows a negligible amount. This is a strong indicator of the scalability of our proposed secure aggregation. Alongside this, the probabilistic optimizations explained in Sec. 3.4 become more beneficial as the model size increases. Compared to a naive implementation where $1 - \mathcal{S}_m$ parameters are checked, we achieve a speedup of 3 orders of magnitude in client and server runtime.

Dataset	Baseline (ms)	zPROBE (ms)
MNIST	208.0	444.7
F-MNIST	214.4	452.9
CIFAR-10	231.2	461.2

Table 2: zPROBE runtime vs. the baseline secure aggregation of (Bell et al. 2020) with no support for Byzantine clients.

We also provide the detailed breakdown of the runtime for various components of zPROBE in Fig. 4. Results are gathered on CIFAR-10 dataset and ResNet-20 architecture with $n = 50$, $c = 7$, and $\mathcal{S}_m = 0.3$. Step 2 has very low overhead, even when only 30% of model updates are Byzantine, which requires more checks. The most significant operation in terms of percent increase from baseline is observed in Step 3 (R2), where the correctness of masked updates are checked (Alg. 1 Round 2 and Alg. 2). zPROBE enjoys a low communication overhead as well, requiring only 2.1MB and 4.4MB of client and server communication respectively, for a round of aggregation over CIFAR-10. Overall, with sub-second per-

¹Raw accuracy numbers are not reported for BREA, therefore, direct comparison is not possible.

²Note that this work focuses on plaintext robust training and does not provide secure aggregation.

formance on all benchmarks examined, zPROBE provides an efficient full privacy-preserving and robust solution for FL.

zPROBE Complexity. In this section we present the complexity analysis of zPROBE runtime with respect to number of clients n (with $k = \log n$) and model size l .

- **Client:** Each client computation consists of performing key agreements with $O(k)$, generating pairwise masks with $O(k \cdot l)$, creating t-out-of-k Shamir shares with $O(k^2)$, performing correctness checks of Alg. 2 with $O(k \cdot l)$, and performing robustness checks of Alg. 3 with $O(l)$. The complexity of client compute is therefore $O(\log^2 n + l \cdot \log n)$.

- **Server:** The server computation consist of reconstructing t-out-of-k shamir shares with $O(n \cdot k^2)$, generating pairwise masks for dropped out clients with $O(n \cdot k \cdot l)$, performing correctness checks of Alg. 2 with $O(n \cdot l)$, and performing robustness checks of Alg. 3 with $O(n \cdot l)$. The overall complexity of server compute is thus $O(n \cdot \log^2 n + n \cdot l \cdot \log n)$.

We are unable to directly compare zPROBE’s runtime numbers with previous private and robust FL methods since their implementations are not publicly available. Instead, Tab. 3 presents a complexity comparison between zPROBE, BREA (So et al. 2020), and EIFFeL (Chowdhury et al. 2021) with respect to number of clients n (with $k = \log n$), model size l , and number of malicious clients m . zPROBE enjoys a lower computational complexity compared to both prior art for client and server. Specifically, the client runtime is quadratic and linear with number of clients in BREA and EIFFeL respectively, whereas logarithmic in zPROBE.

	Client	Server
BREA	$O(n^2 l + n l k^2)$	$O((n^3 + n l) k^2 \cdot \log(k))$
EIFFeL	$O(m n l)$	$O((n + l) n k^2 \cdot \log(k) + m \cdot l \cdot \min(n, m^2))$
zPROBE	$O(k^2 + k l)$	$O(n k^2 + n l k)$

Table 3: Runtime complexity of zPROBE vs. prior works BREA (So et al. 2020) and EIFFeL (Chowdhury et al. 2021).

4.4 Discussion

We perform a sensitivity analysis to various attack parameters and FL configurations on F-MNIST. Number of clients is set to $n = 50$ with $c = 7$ clusters, unless otherwise noted. Sign flip attack (Damaskinos et al. 2018) is applied to all model updates with $\kappa = 5$. As shown, zPROBE is largely robust to changes in the underlying attack or training configuration, consistently recovering the central models’ accuracy.

Portion of Compromised Updates S_m . We vary the portion of Byzantine model updates (S_m) and show the accuracy of the central model with and without zPROBE robustness checks in Fig. 5(a). Even when only a small portion of model updates are malicious, zPROBE’s outlier detection can successfully recover the accuracy from random guess (10%) to 97.9%. To worsen the central model’s accuracy, Byzantine workers are incentivized to attack a high number of model updates. Attacking all model updates results in a 89.7% drop of accuracy when no defense is present. However, even when all model updates are compromised, zPROBE recovers the central model’s accuracy with less than 0.5% error margin.

Attack Magnitude. We control the magnitude of the perturbation applied to model updates by changing the parameter κ in various Byzantine attack scenarios. Fig. 5(b) shows the effect of the attack magnitude on the central model’s accuracy and zPROBE’s defense performance. As seen, a higher perturbation is easier to detect using our median-based robustness check. The Byzantine attack can cause an accuracy drop of $\sim 88\%$ when no robustness check is applied. However, zPROBE can largely recover the accuracy degradation, reducing the accuracy loss to 0.2%-9.8%.

Aggregation Strategy. Recall from Fig. 1 that zPROBE uses the median of per-cluster means (in plaintext) to extract a threshold, which is then used in step 2 to filter out malicious clients. Rather than performing steps 2 and 3 of zPROBE, an alternative robust aggregation rule may directly use the median value to update the global model. Merely using the median for the final aggregation ignores beneficial updates by benign users. This leads to a drastic accuracy degradation of 28.6% compared to zPROBE which includes all gradients that pass the threshold. A comparison between median-based aggregation and zPROBE is presented in Appendix G, Fig. 8.

Number of Clients (n). Fig. 5(c) shows the convergence of zPROBE during training for various $n \in [30, 200]$. We note that n is the subset of clients which are picked for an aggregation round. We pick this range according to practical deployments of FL where the server picks a small fraction of all FL clients for each aggregation round (Shejwalkar et al. 2022). As seen, client count does not affect zPROBE convergence and the central model’s final accuracy. Specifically, zPROBE can scale to $n = 200$, which is among the largest studied user counts in robust and private FL.

Number of Clusters (c). Fig. 5(d) shows the effect of number of clusters on accuracy. The performance of zPROBE is largely independent of the number of clusters, showing less than 0.18% variation for different c while the increase in latency is less than 8%. The number of clusters can therefore be selected freely such that user privacy is ensured. Recall from Fig. 1 that cluster means in step 1 of zPROBE are revealed to the server. To analyze the privacy implications, we rely on the contemporary literature in model/gradient inversion which show that increasing the batch size, or equivalently number of users, (> 100 (Geiping et al. 2020) or > 48 (Yin et al. 2021)) reduces the effectiveness of such attacks.

We benchmark the SOTA attack by Geiping et al. (2020) to reconstruct user data from the aggregate. We use a small 4-layer model and a batch size of 10 to benefit the attacker. Fig. 10(a),(b) in Appendix I show the efficacy of the inversion attack as the number of users in the aggregation varies. As seen, the reconstructions are unintelligible with > 4 users per cluster. More recently Elkordy et al. (2022) quantify the user information leakage from the aggregate value using Mutual Information (MI). They show that MI reduces with more clients, starting to plateau around 10-20 users where the reconstructed image quality of the DLG attack (Zhu et al. 2019) is severely affected. Based on these results, our cluster size range of 7 to 30 can preserve user privacy.

User Dropout. zPROBE secure aggregation supports user dropouts, i.e., when a user is disconnected amidst training iterations and/or in between zPROBE steps (see Fig. 1). We

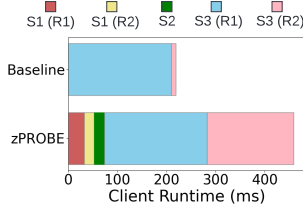


Figure 4: Runtime breakdown for CIFAR-10, corresponding to rounds (R) from Alg. 1 and steps (S) from Fig. 1.

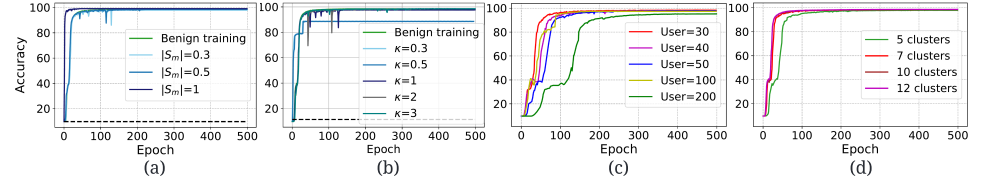


Figure 5: Ablation studies on zPROBE defense performance with varying (a) portion of compromised gradients, (b) attack magnitude, (c) number of clients, and (d) number of user clusters. The dashed line in (a), (b) corresponds to the highest test accuracy obtained during training when no defense is applied.

simulate the effect of user dropout on the training accuracy of zPROBE in Appendix H, Fig. 9. As shown, the changes in the training accuracy are very subtle ($< 0.13\%$ difference) in the presence of random user dropouts.

5 Related Work

Secure Aggregation. Cryptographic techniques have been used in prior work for secure aggregation, e.g., by using random masks to hide private updates (Bonawitz et al. 2017; Bell et al. 2020) during computation. A line of work (Corrigan-Gibbs and Boneh 2017; Nguyen et al. 2022) considers a different trust model with non-colluding servers that receive secret shares of data and collaborate to compute the aggregate. However, realizing the non-colluding trust assumption can be challenging in practice. Differential Privacy (DP) can provide complementary privacy guarantees to cryptographic methods (by protecting information leakage from output), and have been used in conjunction to reduce the required noise. Truex et al. (2019) combine threshold homomorphic encryption and differential privacy for private aggregation.

Robust Aggregation. Prior work on Byzantine-robust aggregation sanitizes the client updates using robust statistics or historical information. (Multi-)Krum (Blanchard et al. 2017; Damaskinos et al. 2019) selects updates with minimum Euclidean distance to their neighbors. Coordinate-wise operations based on median and trimmed mean (Yin et al. 2018; Xie et al. 2018a) have also been proposed that calculate the mean of values closest to the median for each coordinate. More recently, AKSEL (Boussetta et al. 2021) defines an interval around the median and aggregates the values within that interval. (Chen et al. 2017; Pillutla et al. 2019) use the robustness of geometric median (generalized to multiple dimensions), to provide a robust update rule. Bulyan (Guerraoui et al. 2018) augments prior aggregation rules to ensure all coordinates are agreed upon by a majority of user gradients.

Several works propose applying robust aggregation over an accumulated history of gradients, assuming IID data. Allen-Zhu et al. (2020) use the concentration of aggregated past gradients around the median to mark byzantine workers. Similarly, El Mhamdi et al. (2021) apply Byzantine-resilient aggregation rules on a weighted average of past gradients using a momentum term. In lieu of using the median, centered clipping (Karimireddy et al. 2021) iteratively scales the accumulated gradients to ensure robust aggregation. The

aforesaid works focus on robust aggregation under IID data assumptions. Karimireddy et al. (2022) propose user clustering as an effective way to adapt previously proposed robust aggregation methods, e.g., Krum, to heterogeneous (non-IID) data. zPROBE designs a *new* aggregation rule that 1) enables efficient execution in the secure domain and 2) achieves state-of-the-art accuracy compared to (Karimireddy et al. 2022).

Robust and Secure Aggregation. RoFL (Burkhalter et al. 2021) focuses on model poisoning, when malicious users try to embed a backdoor in the model, without downgrading accuracy on benign data. RoFL uses Pedersen commitments to implement ZKP of norm bounds over model updates. RoFL does not support dropouts during aggregation and the proposed l -norm bounds are unsuitable against Byzantine workers. zPROBE considers Byzantine attacks where the malicious parties send invalid updates to degrade the central model’s accuracy. In this domain, BREA (So et al. 2020) relies on Shamir secret sharing and multi-Krum (Damaskinos et al. 2019) for aggregation. However, BREA reveals the pairwise distances of client updates to the server, i.e., even one client’s collusion with the server would reveal all updates.

SHARE (Velicheti et al. 2021) incorporates secure averaging (Bonawitz et al. 2017) on randomly clustered clients, and filters cluster averages through robust aggregation. Any cluster with malicious clients detected will be dropped, resulting in loss of all benign updates. SHARE’s mitigation is to repeat the random clustering several times for each epoch, which results in increased computation and communication cost. Moreover, reclustering compromises privacy as the server observes different variations of cluster averages which can leak information about the user updates. Most recently, EIFFeL (Chowdhury et al. 2021) proposes a robust aggregation using Shamir shares of client updates, and secret-shared non-interactive proofs (SNIP). EIFFeL does not support rank-based statistics for robustness checks, resulting in higher accuracy degradation, and requires access to a clean public dataset for defense parameters.

6 Conclusion

This paper presented zPROBE, a novel framework for low overhead, scalable, private, and robust FL in the malicious client setting. zPROBE ensures correct behavior from clients, and performs robustness checks on model updates. With a combination of zero-knowledge proofs and secret sharing

techniques, `zPROBE` provides robustness guarantees without compromising client privacy. `zPROBE` presents a paradigm shift from previous work by providing a private robustness defense relying on rank-based statistics with cost that grows sublinearly with respect to number of clients.

References

- Allen-Zhu, Z.; Ebrahimiaghazani, F.; Li, J.; and Alistarh, D. 2020. Byzantine-Resilient Non-Convex Stochastic Gradient Descent. In *International Conference on Learning Representations*.
- Baruch, G.; Baruch, M.; and Goldberg, Y. 2019. A Little Is Enough: Circumventing Defenses For Distributed Learning. *Advances in Neural Information Processing Systems*, 32: 8635–8645.
- Bell, J. H.; Bonawitz, K. A.; Gascón, A.; Lepoint, T.; and Raykova, M. 2020. Secure single-server aggregation with (poly) logarithmic overhead. In *Proceedings of the 2020 ACM SIGSAC Conference on Computer and Communications Security*, 1253–1269.
- Bhagoji, A. N.; Chakraborty, S.; Mittal, P.; and Calo, S. 2019. Analyzing federated learning through an adversarial lens. In *International Conference on Machine Learning*, 634–643. PMLR.
- Blanchard, P.; El Mhamdi, E. M.; Guerraoui, R.; and Stainer, J. 2017. Machine learning with adversaries: Byzantine tolerant gradient descent. In *Proceedings of the 31st International Conference on Neural Information Processing Systems*, 118–128.
- Bonawitz, K.; Ivanov, V.; Kreuter, B.; Marcedone, A.; McMahian, H. B.; Patel, S.; Ramage, D.; Segal, A.; and Seth, K. 2017. Practical secure aggregation for privacy-preserving machine learning. In *proceedings of the 2017 ACM SIGSAC Conference on Computer and Communications Security*, 1175–1191.
- Boussetta, A.; El-Mhamdi, E.-M.; Guerraoui, R.; Maurer, A.; and Rouault, S. 2021. AKSEL: Fast Byzantine SGD. In *24th International Conference on Principles of Distributed Systems (OPODIS 2020)*.
- Burkhalter, L.; Lycklama, H.; Viand, A.; Küchler, N.; and Hithnawi, A. 2021. RoFL: Attestable Robustness for Secure Federated Learning. *arXiv preprint arXiv:2107.03311*.
- Chen, Y.; Su, L.; and Xu, J. 2017. Distributed statistical machine learning in adversarial settings: Byzantine gradient descent. *Proceedings of the ACM on Measurement and Analysis of Computing Systems*, 1(2): 1–25.
- Chowdhury, A. R.; Guo, C.; Jha, S.; and van der Maaten, L. 2021. EIFFeL: Ensuring Integrity for Federated Learning. *arXiv preprint arXiv:2112.12727*.
- Corrigan-Gibbs, H.; and Boneh, D. 2017. Prio: Private, robust, and scalable computation of aggregate statistics. In *14th USENIX Symposium on Networked Systems Design and Implementation (NSDI 17)*, 259–282.
- Damaskinos, G.; El Mhamdi, E. M.; Guerraoui, R.; Guirguis, A. H. A.; and Rouault, S. L. A. 2019. Aggregathor: Byzantine machine learning via robust gradient aggregation. In *The Conference on Systems and Machine Learning (SysML), 2019, CONF*.
- Damaskinos, G.; Guerraoui, R.; Patra, R.; Taziki, M.; et al. 2018. Asynchronous Byzantine machine learning (the case of SGD). In *International Conference on Machine Learning*, 1145–1154. PMLR.
- Damgård, I.; Pastro, V.; Smart, N.; and Zakarias, S. 2012. Multiparty computation from somewhat homomorphic encryption. In *Annual Cryptology Conference*, 643–662. Springer.
- Diffie, W.; and Hellman, M. 1976. New directions in cryptography. *IEEE transactions on Information Theory*, 22(6): 644–654.
- El Mhamdi, E. M.; Guerraoui, R.; and Rouault, S. L. A. 2021. Distributed momentum for byzantine-resilient stochastic gradient descent. In *9th International Conference on Learning Representations (ICLR), CONF*.
- Elkordy, A. R.; Zhang, J.; Ezzeldin, Y. H.; Psounis, K.; and Avestimehr, S. 2022. How Much Privacy Does Federated Learning with Secure Aggregation Guarantee? *arXiv preprint arXiv:2208.02304*.
- Geiping, J.; et al. 2020. Inverting gradients-how easy is it to break privacy in federated learning? *NeurIPS*.
- Guerraoui, R.; Rouault, S.; et al. 2018. The hidden vulnerability of distributed learning in byzantium. In *International Conference on Machine Learning*, 3521–3530. PMLR.
- He, K.; Zhang, X.; Ren, S.; and Sun, J. 2016. Deep residual learning for image recognition. In *Proceedings of the IEEE conference on computer vision and pattern recognition*, 770–778.
- Karimireddy, S. P.; He, L.; and Jaggi, M. 2021. Learning from history for byzantine robust optimization. In *International Conference on Machine Learning*, 5311–5319. PMLR.
- Karimireddy, S. P.; He, L.; and Jaggi, M. 2022. Byzantine-Robust Learning on Heterogeneous Datasets via Bucketing. In *International Conference on Learning Representations*.
- Krizhevsky, A.; Nair, V.; and Hinton, G. 2010. Cifar-10 (canadian institute for advanced research). URL <http://www.cs.toronto.edu/kriz/cifar.html>, 5.
- LeCun, Y. 1998. The MNIST Database. <http://yann.lecun.com/exdb/mnist/>.
- LeCun, Y.; Bottou, L.; Bengio, Y.; and Haffner, P. 1998. Gradient-based learning applied to document recognition. *Proceedings of the IEEE*, 86(11): 2278–2324.
- Melis, L.; Song, C.; De Cristofaro, E.; and Shmatikov, V. 2019. Exploiting unintended feature leakage in collaborative learning. In *2019 IEEE Symposium on Security and Privacy (SP)*, 691–706. IEEE.
- Nguyen, T. D.; Rieger, P.; Chen, H.; Yalame, H.; Möllering, H.; Fereidooni, H.; Marchal, S.; Miettinen, M.; Mirhoseini, A.; Zeitouni, S.; Koushanfar, F.; Sadeghi, A.-R.; and Schneider, T. 2022. FLAME: Taming Backdoors in Federated Learning. *31st USENIX Security Symposium (USENIX Security 22)*.

Pillutla, K.; Kakade, S. M.; and Harchaoui, Z. 2019. Robust aggregation for federated learning. *arXiv preprint arXiv:1912.13445*.

Rieke, N.; Hancox, J.; Li, W.; Milletari, F.; Roth, H. R.; Albarqouni, S.; Bakas, S.; Galtier, M. N.; Landman, B. A.; Maier-Hein, K.; et al. 2020. The future of digital health with federated learning. *NPJ digital medicine*, 3(1): 1–7.

Shamir, A. 1979. How to share a secret. *Communications of the ACM*, 22(11): 612–613.

Shejwalkar, V.; Houmansadr, A.; Kairouz, P.; and Ramage, D. 2022. Back to the drawing board: A critical evaluation of poisoning attacks on production federated learning. In *2022 IEEE Symposium on Security and Privacy (SP)*, 1354–1371. IEEE.

So, J.; Güler, B.; and Avestimehr, A. S. 2020. Byzantine-resilient secure federated learning. *IEEE Journal on Selected Areas in Communications*.

Truex, S.; Baracaldo, N.; Anwar, A.; Steinke, T.; Ludwig, H.; Zhang, R.; and Zhou, Y. 2019. A hybrid approach to privacy-preserving federated learning. In *Proceedings of the 12th ACM Workshop on Artificial Intelligence and Security*, 1–11.

Velicheti, R. K.; Xia, D.; and Koyejo, O. 2021. Secure Byzantine-Robust Distributed Learning via Clustering. *arXiv preprint arXiv:2110.02940*.

Wang, X. accessed 2022. EMP-Toolkit. <https://github.com/emp-toolkit>.

Weng, C.; Yang, K.; Katz, J.; and Wang, X. 2021a. Wolverine: fast, scalable, and communication-efficient zero-knowledge proofs for boolean and arithmetic circuits. In *2021 IEEE Symposium on Security and Privacy (SP)*, 1074–1091. IEEE.

Weng, C.; Yang, K.; Xie, X.; Katz, J.; and Wang, X. 2021b. Mystique: Efficient Conversions for {Zero-Knowledge} Proofs with Applications to Machine Learning. In *30th USENIX Security Symposium (USENIX Security 21)*, 501–518.

Xiao, H.; Rasul, K.; and Vollgraf, R. 2017. Fashion-mnist: a novel image dataset for benchmarking machine learning algorithms. *arXiv preprint arXiv:1708.07747*.

Xie, C.; Koyejo, O.; and Gupta, I. 2018a. Generalized byzantine-tolerant sgd. *arXiv preprint arXiv:1802.10116*.

Xie, C.; Koyejo, O.; and Gupta, I. 2018b. Phocas: dimensional byzantine-resilient stochastic gradient descent. *arXiv preprint arXiv:1805.09682*.

Xu, J.; Glicksberg, B. S.; Su, C.; Walker, P.; Bian, J.; and Wang, F. 2021. Federated learning for healthcare informatics. *Journal of Healthcare Informatics Research*, 5(1): 1–19.

Yang, W.; Zhang, Y.; Ye, K.; Li, L.; and Xu, C.-Z. 2019. Ffd: A federated learning based method for credit card fraud detection. In *International conference on big data*, 18–32. Springer.

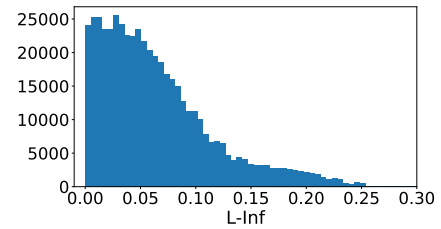
Yin, D.; Chen, Y.; Kannan, R.; and Bartlett, P. 2018. Byzantine-robust distributed learning: Towards optimal statistical rates. In *International Conference on Machine Learning*, 5650–5659. PMLR.

Yin, H.; et al. 2021. See through gradients: Image batch recovery via gradinversion. In *CVPR*.

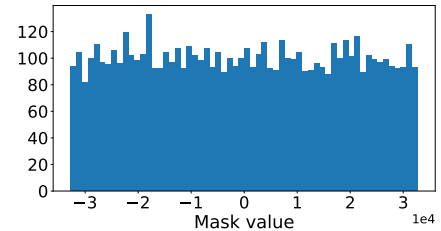
Zhu, L.; Liu, Z.; and Han, S. 2019. Deep leakage from gradients. *Advances in neural information processing systems*, 32.

A Malicious Seed Modification

Fig. 6(a) demonstrates the histogram of L_∞ norm of *benign* gradients, observed throughout training across 100 users for CIFAR-10 dataset. As seen, majority of the gradient norms are bounded in $[0, 0.25]$. Masks are generated using seeds through a pseudorandom generator (PRG), and malicious users cannot control the resulting error when changing the seed. Fig. 6(b) shows a histogram of mask values generated from random seeds over 10000 runs. As shown, changing the seed may cause unpredictable and drastic changes in the mask. By changing the random seed, the generated masks can vary anywhere between -3×10^4 to 3×10^4 , which is much larger than the normal observed range for model updates. As such, when a malicious user changes the random seed from which the masks are generated, it can lead to easily recognizable errors in the gradient that raises alarms for the server. Thus, in our threat model malicious users are incentivized to use the correct seed when computing masks.



(a)



(b)

Figure 6: Histogram of (a) ResNet-20 gradient norms observed during training on CIFAR-10, and (b) mask values when changing the random seed.

B Experimental Setup Details

Dataset and Models. We consider three benchmarks commonly studied by prior work in secure FL. Our first benchmark is a variant of LeNet5 (LeCun et al. 1998) trained on the MNIST dataset (LeCun 1998), with 2 convolution and 3 fully-connected layers, totaling 42K parameters. Our second

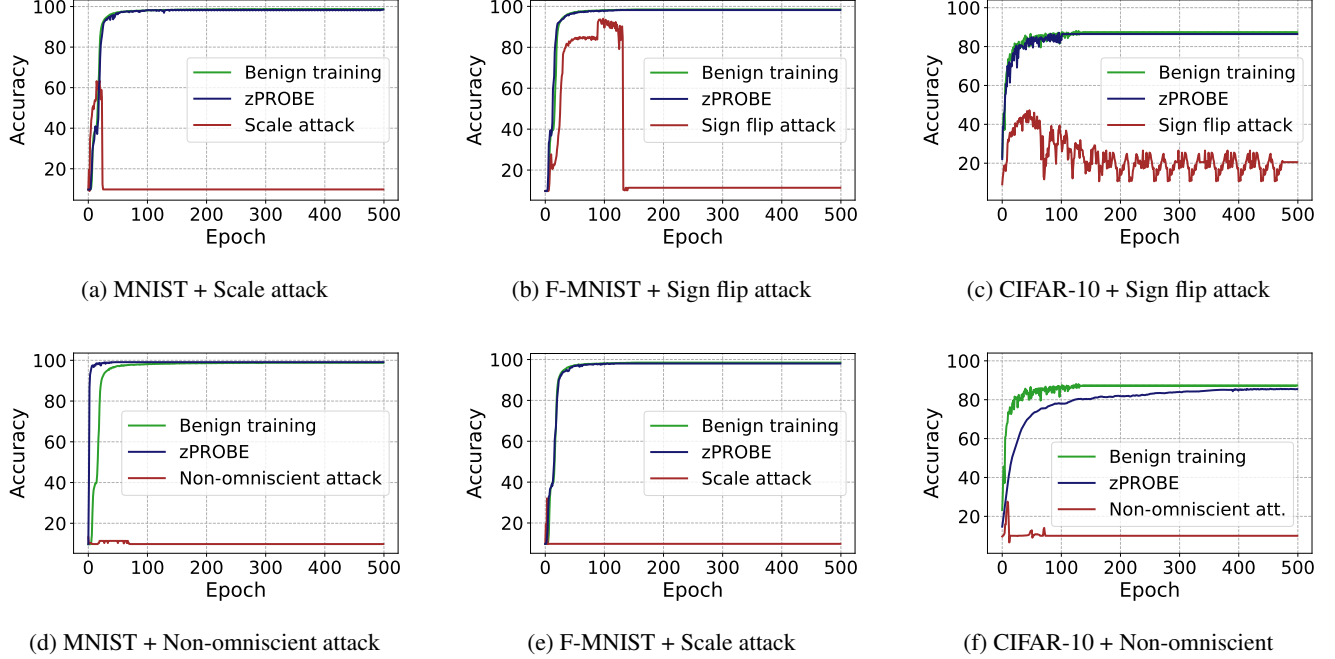


Figure 7: Test accuracy as a function of FL training epochs for different attacks and benchmarks. Each plot shows the benign training (green), Byzantine training without defense (maroon), and Byzantine training in the presence of zPROBE defense.

benchmark is the Fashion-MNIST (F-MNIST) dataset (Xiao et al. 2017) trained on the LeNet5 architecture with 60K parameters. Finally, to showcase the scalability of our approach, we evaluate ResNet-20 (He et al. 2016) with 273K parameters trained on the CIFAR-10 dataset (Krizhevsky et al. 2010) which is among the biggest benchmarks studied in the secure FL literature (Burkhalter et al. 2021; Chowdhury et al. 2021). Table 4 encloses the training hyperparameters for all models.

Benchmark	# Clients	LR	# Epochs	Batch size (per user)
MNIST (IID) + LeNet5	50	0.01	500	12800 (256)
MNIST (non-IID) + LeNet5	25	0.01	500	800 (32)
F-MNIST (IID) + LeNet5	50	0.01	500	12800 (256) [†]
CIFAR-10 (IID) + ResNet-20	50	0.05	500	12800 (256)

[†]When varying the number of clients, we keep the total batch size as 12800 and scale the per user batch size accordingly.

Table 4: Training hyperparameters.

Implementation and Configuration. zPROBE defense is implemented in Python and integrated in PyTorch to enable model training. We use the EMP-Toolkit (Wang accessed 2022) for implementation of zero-knowledge proofs. We run all experiments on a 128GB RAM, AMD Ryzen 3990X CPU desktop. All reported runtimes are averaged over 100 trials.

C Byzantine Attacks

We show the effectiveness of our robustness checks against three commonly used Byzantine attacks. Here \mathcal{U}_m denotes the malicious updates, where $|\mathcal{U}_m| = \mathcal{S}_m \cdot l$ and l is the total number of model updates.

- *Sign Flip* (Damaskinos et al. 2018). Malicious client flips the sign of the update: $u = -\kappa \cdot u, \kappa > 0 (\forall u \in \mathcal{U}_m)$
- *Scaling* (Bhagoji et al. 2019). Malicious client scales the local gradients to increase the influence on the global model: $u = \kappa \cdot u, \kappa > 0 (\forall u \in \mathcal{U}_m)$
- *Non-omniscient attack* (Baruch et al. 2019). Malicious clients construct their Byzantine update by adding a scaled Gaussian noise to their original update with mean μ and standard deviation σ : $u = \mu - \kappa \cdot \sigma (\forall u \in \mathcal{U}_m)$

D zPROBE Test Accuracy

Fig. 7 shows the test accuracy of zPROBE in face of different variations of Byzantine attacks and datasets. The dataset is distributed evenly (IID) among $n = 50$ clients. The server randomly clusters users into $c = 7$ groups during each training round. We assume malicious users compromise all model updates $|\mathcal{S}_m| = 1$ to maximize the accuracy degradation.

E Effect of \mathcal{S}_m on zPROBE Runtime

Tab. 5 summarizes the runtime of zPROBE versus the portion of attacked model updates. By decreasing \mathcal{S}_m , zPROBE requires more checks to detect the outlier gradients as outlined in Eq. 2. Nevertheless, due to the optimizations in zPROBE robustness and correctness checks, we are still able to maintain sub-second runtime and sublinear growth with respect to number of ZKP checks necessary.

	0.1	0.3	\mathcal{S}_m 0.5	0.7	1.0
# ZKP Checks	51	15	8	5	1
zPROBE Runtime (ms)	777.9	452.9	372.6	349.6	316.5

Table 5: zPROBE performance for LeNet5 on F-MNIST vs. the portion of Byzantine model updates (\mathcal{S}_m).

F Effect of Number of Clients on zPROBE Runtime

Fig 6 shows the effect of increasing the number of clients on the performance on zPROBE. For these experiments, results are gathered on the F-MNIST dataset, with $c = 7$ and $|\mathcal{S}_m| = 0.3$. As seen, although exceeding the sub-second performance as the number of clients scales up, zPROBE maintains sublinear growth in runtime with respect to number of clients.

# Clients	zPROBE Runtime (ms)
30	298.4
40	369.7
50	452.9
70	598.8
100	828.6
200	1620.4

Table 6: Runtime of zPROBE over varying number of clients

G Effect of Aggregation Method on Accuracy

zPROBE leverages the median of averaged model updates across user clusters to check whether the incoming updates are benign or Byzantine. An alternative aggregation strategy is to directly use the median of cluster means, rather than performing the subsequent per-user checks. Fig. 8 shows the test accuracy of zPROBE as training progresses, when compared to the above baseline aggregation method that applies the coordinate-wise median of cluster means. As seen, compared to zPROBE, this baseline suffers from a large accuracy degradation, since all information in benign user updates is lost by replacing the aggregation with the median, which can potentially contain Byzantine workers.

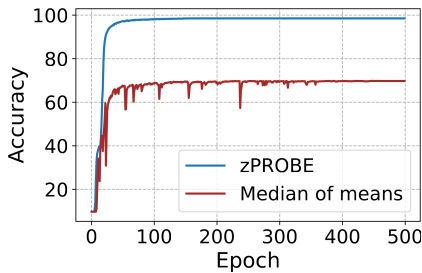


Figure 8: Test accuracy of zPROBE compared with an aggregation methodology that uses the median of cluster means to update the model.

H Effect of User Dropout

Fig 9 shows the effect of random user dropouts on zPROBE defense. As shown, the fluctuations in the central model’s test accuracy are negligible ($< 0.13\%$). The robustness of zPROBE aggregation protocol to user dropouts is intuitive since the remaining users can carry on the training.

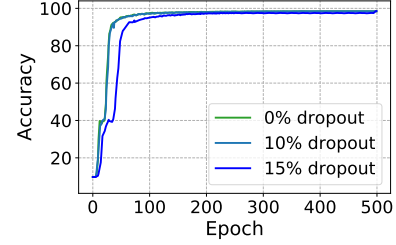


Figure 9: The effect of (a) number of clusters, and (b) user dropout on defense.

I Effect of Cluster Size on Inversion Attack

Fig. 10 shows the effect of cluster size on gradient inversion attacks. In Fig 10(a) we show the effectiveness of the attack (Geiping et al. 2020) for different cluster sizes. Fig 10(b) represents the reconstruction results from user data for different number of users participating in the aggregation round.

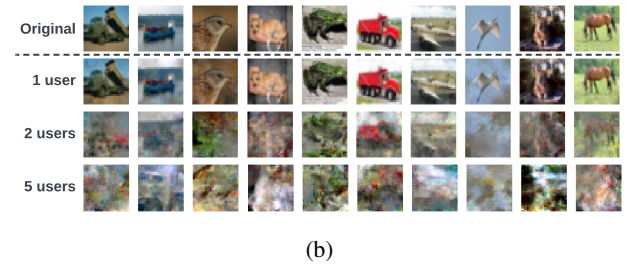
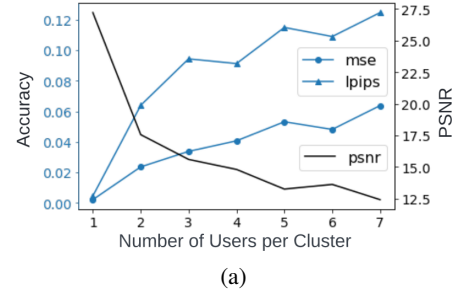


Figure 10: Performance of gradient inversion attacks for different cluster sizes.